Multi-Variable Relations for Soil Effects on Peak Seismic Motion Parameters

GEORGE D. BOUCKOVALAS
Professor N.T.U.A.

ACHILLEAS G. PAPADIMITRIOU
Dr Civil Engineer N.T.U.A.

Abstract

Soil effects on peak seismic acceleration and velocity are expressed by simple relations, in terms of five (5) basic site and excitation parameters: the fundamental vibration periods of the soil T_S and the bedrock T_b, the predominant excitation period T_e, the peak seismic acceleration at outcropping bedrock a^b_{max} and the number of significant cycles n. Furthermore, relations are proposed for the estimation of T_S in terms of the soil thickness H, the average shear wave velocity of the soil $V_{S,o}$ and a^b_{max}. All relations were established in two steps: (a) the basic parameters were first identified through a simplified analytical simulation of the site excitation, and (b) the effect of each parameter was subsequently estimated from a statistical analysis of relevant data from more than 700 one-dimensional equivalent-linear seismic ground response analyses. The soil profiles used in the numerical analyses correspond to natural sites, while the seismic excitations originate from actual seismic motion recordings. Comparison with strong motion recordings, from seven (7) case studies, shows that the accuracy of the proposed relations is comparable to that of the equivalent-linear method. Hence they can be readily used as a quick alternative for routine applications, as well as for spreadsheet computations (e.g. GIS-aided seismic microzonation studies) where the more accurate numerical methods are cumbersome to implement.

1. INTRODUCTION

Soil alters the characteristics of seismic waves, in such a way that the amplitude as well as the frequency content of seismic motions on the free soil surface and on the free surface of the bedrock is different. Although it is well understood today that the topography of the ground and that of the bedrock basin are sometimes equally important for the definition of seismic ground motions, soil effects are the first to be considered in practical applications.

In broad terms, the methods used for this purpose may be divided into two categories:

a) Empirical, which correlate seismic motion characteristics from actual recordings with soil conditions at the recording site. Soil conditions are commonly characterized either in pure geological terms (e.g. [15], [6], [1], [24]) or with the aid of some representative soil parameter such as the average shear wave velocity (e.g. [19], [9], [7], [8]).

b) Numerical, which employ wave propagation theory either in the frequency or in the time domain and may simulate the details of any given soil profile and seismic excitation (e.g. [14], [17], [18], [22]).

Currently available empirical methods offer the advantage of immediate and fairly inexpensive application, but often fail to provide the accuracy required for engineering applications [3]. On the other hand, numerical methods are more accurate, but their application to routine projects is limited by the time and cost required in order to collect all necessary input data and to perform the analyses. To fill this gap, a set of relations is established here and in a companion paper [5], which draws upon the theory of 1-D seismic wave propagation in order to identify the basic factors affecting soil response and to evaluate their influence. In practical terms, such relations could prove useful in routine projects, or in cases where numerical methods cannot be easily implemented, such as in seismic microzonation studies of wide areas that are commonly performed with the aid of G.I.S. systems (e.g. [21]).

The new relations are based on data from equivalent-linear site response analyses, performed to simulate actual seismic excitations and natural soil conditions. In this way, the values of all parameters varied within a wide range, making a multivariable regression analysis of the data reliable. To guide the regression analysis, the basic parameters of the relations were first identified by means of an analytical solution for uniform soil and harmonic base excitation. To verify their validity for practical applications, an extensive evaluation is presented here pertaining to comparisons with strong motion data and related numerical analyses for seven (7) case studies.

Submitted: Oct. 30, 2002 Accepted: July 1, 2004

This paper focuses upon soil effects on the peak ground acceleration, the peak ground velocity and the fundamental site period. The effect of soil on elastic response spectra is the subject of a companion paper [5].

2. LIST OF SYMBOLS

$\lvert A_s \rvert$	Amplitude of outcropping bedrock to soil surface amplification ratio
$A_{s,o}$	Complex amplification ratio within soil
$A_{b,o}$	Complex amplification ratio within bedrock
α	Impedance ratio
α^*	Complex impedance ratio
ρ_b	Mass density of bedrock
ρ_s	Mass density of soil column
ξ_b	Critical damping ratio of bedrock
ξ_s	Critical damping ratio of soil column
H	Thickness of soil column
V_s	Shear wave velocity in uniform soil
$V_{s,o}$	Elastic shear wave velocity in uniform soil
V_s^*	Complex shear wave velocity in soil
$\overline{V}_{s,o}$	Average elastic shear wave velocity in soil column
T_s	Fundamental soil period
T_s^*	Complex fundamental soil period
$T_{s,o}$	Fundamental elastic soil period
T_e	Predominant excitation period
V_b	Shear wave velocity in (uniform) bedrock
T_b	Fundamental (uniform) bedrock period (=$4H/V_b$)
k_s	Wave number for soil
k_s^*	Complex wave number for damped soil
$\xi_{e,s}$	Overall damping ratio of soil column
k_b	Wave number for bedrock
a^b_{max}	Peak horizontal acceleration at outcropping bedrock
a^s_{max}	Peak horizontal acceleration at soil surface
A_a	Outcropping bedrock to soil surface peak horizontal acceleration amplification ratio
R_{Aa}	Relative estimation error of A_a
V^b_{max}	Peak horizontal velocity at outcropping bedrock
V^s_{max}	Peak horizontal velocity at soil surface
A_V	Outcropping bedrock to soil surface peak horizontal velocity amplification ratio
R_{Av}	Relative estimation error of A_V
n	Number of equivalent uniform cycles of excitation
γ	Cyclic shear strain amplitude

3. PARAMETER IDENTIFICATION

The basic parameters contributing to soil effects may be identified with the aid of one-dimensional wave propagation theory for a uniform, visco-elastic soil and bedrock profile under harmonic base excitation. Given the algebra outlined in the Appendix, the ratio of the amplitude of motion at the free ground surface to that at the outcropping bedrock is expressed as:

$$\left|A_S\right| = \frac{exp\left[\xi_b \frac{T_b}{T_S}\left(\frac{\pi}{2}\frac{T_S}{T_e}\right)\right]}{\left|cos\left(\frac{\pi}{2}\frac{T_S^*}{T_e}\right) + i\alpha^* \, sin\left(\frac{\pi}{2}\frac{T_S^*}{T_e}\right)\right|} \tag{3.1}$$

where (ρ_S , ξ_S) and (ρ_b , ξ_b) denote the pairs of mass density and damping for the soil and the bedrock, T_S and T_b are the fundamental vibration periods of columns of soil and bedrock of the same thickness H, T_e is the excitation period, $T_S^* = T_S(1-i\xi_S)$, while

$\alpha = \frac{\rho_S}{\rho_b}\frac{T_b}{T_S}$ and $\alpha^* = \alpha\frac{1+i\xi_S}{1-i\xi_S}$.

For small values of the impedance ratio (and the critical damping ratio ξ_S, Eq. (3.1) may be approximated by:

$$\left|A_S\right| = \frac{exp\left[\xi_b \frac{T_b}{T_S}\left(\frac{\pi}{2}\frac{T_S}{T_e}\right)\right]}{\sqrt{cos^2\left(\frac{\pi}{2}\frac{T_S}{T_e}\right) + \left[\xi_{e,S}\left(\frac{\pi}{2}\frac{T_S}{T_e}\right)\right]^2}} \tag{3.2}$$

where

$$\xi_{e,S} = \xi_S + \frac{2}{\pi}\alpha\frac{T_e}{T_S} \tag{3.3}$$

These analytical relations refer to the steady state response of the soil profile. Accounting for the transient phase of the response, the amplification ratio A_S has to be related to the duration of the excitation, or to the number of cycles n. Thus, A_S can be considered overall a function of five independent factors: T_b/T_S, T_S/T_e, ρ_S/ρ_b, ξ_S, ξ_b and n. Furthermore, for non-linear soils, the peak acceleration of the seismic excitation a^b_{max} should be added to the above factors, as it affects both the T_S and the ξ_S of the soil.

In this study, priority is given to the effect of four (4) of these factors: T_S/T_e, T_b/T_S, a^b_{max} and n. The effect of the remaining factors is overlooked since ξ_b and ρ_S/ρ_b show little variability, while ξ_S is mostly a function of earthquake -induced shear strains and, in turn, of a^b_{max} and n.

4. DATABASE AND STATISTICS

The proposed relations are based on a multivariable regression analysis of the input data and the results of more than 700 numerical analyses of seismic ground response. The site model used for these analyses consists of a number of horizontal soil layers, with non-linear visco-elastic response, resting upon a uniform, linear visco-elastic bedrock. Computations follow the equivalent-linear method, assuming vertical propagation of earthquake-induced shear

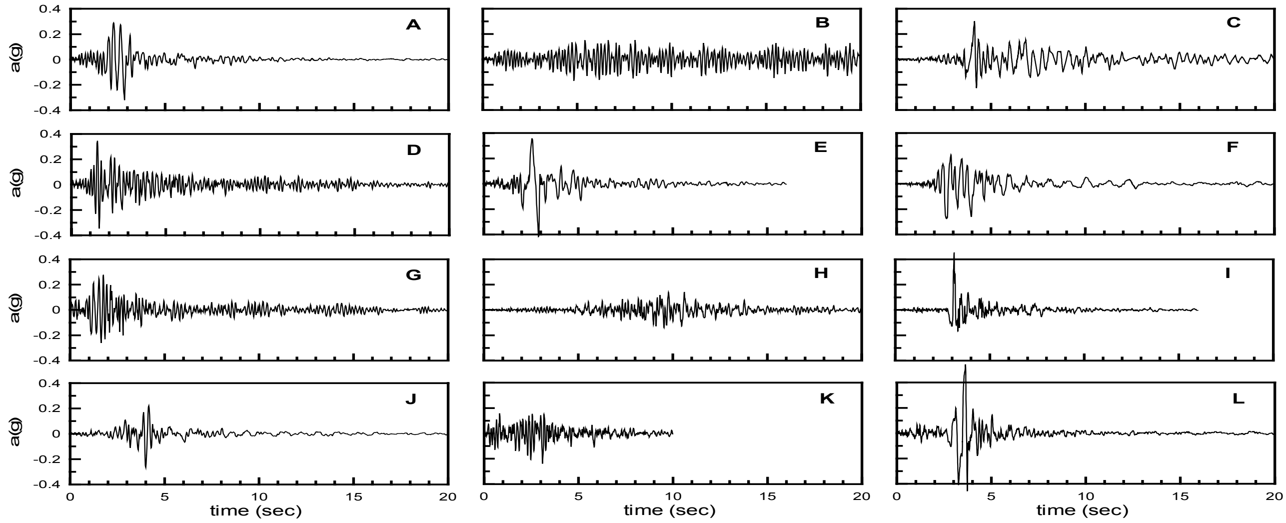

Figure 1: Acceleration time histories of seismic excitations used in the equivalent linear numerical analyses.
Σχήμα 1: Χρονοϊστορίες επιτάχυνσης που χρησιμοποιήθηκαν στις ισοδύναμα γραμμικές αριθμητικές αναλύσεις.

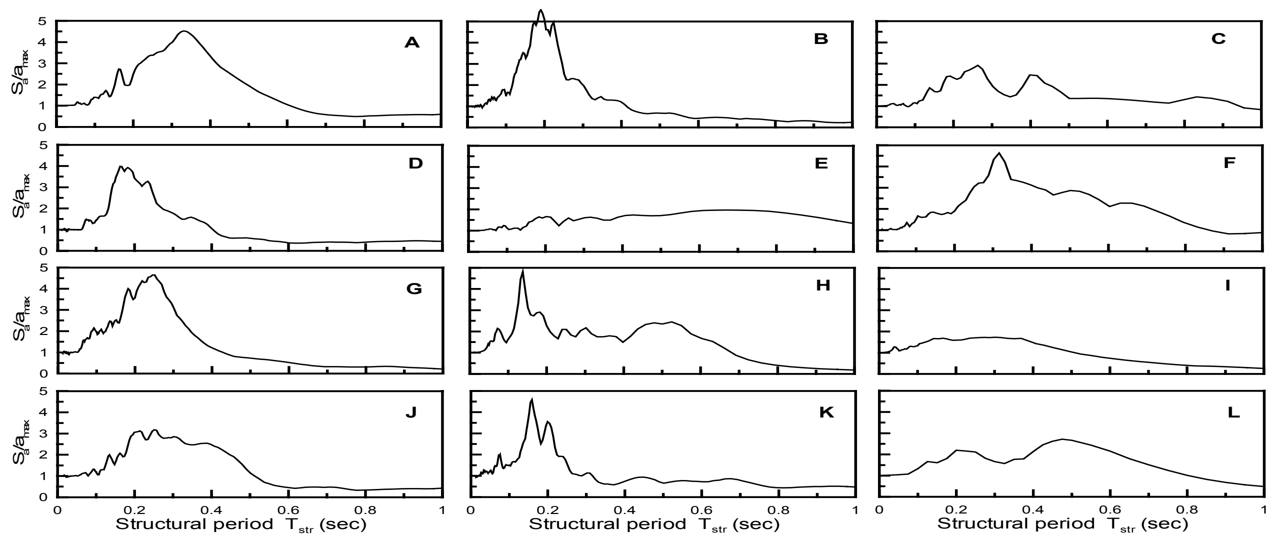

Figure 2: Elastic response spectra (5% damping) of excitations used in the equivalent linear numerical analyses.
Σχήμα 2: Ελαστικά φάσματα απόκρισης (απόσβεση 5%) των διεγέρσεων των ισοδύναμα-γραμμικών αριθμητικών αναλύσεων.

waves from the seismic bedrock to the ground surface and vice-versa [22, 14]. This method has been the standard analysis tool worldwide for a long time, and consequently its advantages and limitations are better understood than those of alternative true non-linear approaches (e.g. [17], [18]). Furthermore, its overall accuracy for low and moderate levels of ground shaking has been directly or indirectly demonstrated in a number of recent case studies, through comparison with data from seismic array recordings (e.g. [11], [20], [10], [12], [23]).

The more than 700 equivalent linear analyses were performed using 12 different (base-line corrected) seismic records as outcropping bedrock excitations. The characteristics of the recordings are presented in Table 1 and in Figures 1 and 2. No alteration was introduced to the records, other than the scaling to the desired value of a^b_{max} per analysis, depending on the project at hand. Defining as predominant period T_e of the excitation the period for which its spectral acceleration S_a (for 5% critical damping ratio) takes its peak value, observe that T_e in the excitations used varies from 0.1 to 0.8 sec, capturing a wide spectrum of potential seismic events.

For each excitation, n was estimated as the number of cycles in the time-history that exceed a level of acceleration equal to $a^b_{max}(M\text{-}1)/10$, where M is the earthquake magnitude. This empirical "rule of thumb" is an extension of the relation between equivalent uniform and maximum shear strains adopted in the numerical analyses of seismic ground response [14]. Observe that for the excitations used, n = 0.5 to 24, again capturing a wide spectrum of potential seismic events.

In the majority of the analyses, the seismic bedrock was defined within Neogene or older geological formations, with shear wave velocity V_b = 550m/s and ρ_b=2.2Mg/m^3.

The analyses were performed for 105 soil sites where geotechnical investigations were available, including measurements (mainly crosshole) of shear wave velocity, as part of major infrastructure development projects in Greece (e.g. microzonation studies, design of motorways, gas and oil transmission pipelines). Each site was usually analyzed for 2 to 4 excitations and 1 to 2 levels of a^b_{max}, depending on the project at hand.

Soil non-linearity was introduced in terms of the shear modulus degradation and hysteretic damping ratio curves [25], for soils of different plasticity (e.g. Fig. 9). With few exceptions, the soil profiles considered in this study consisted of cohesionless non-plastic sand, silt or gravel, as well as of low plasticity clays and marls. Hence the theoretical predictions refer to soil layers of plasticity index between 0 and 50%. Such soils exhibit a higher potential for non-linearity relative to more plastic clays.

The overall variability of the site conditions is outlined in Table 2, by means of the range and frequency distribution of the major site characteristics. In addition, this table provides the range and frequency distribution of the main parameters that affect soil amplification, namely: T_S/T_e, T_b/T_S, α^b_{max} and n.

Table 1: Characteristics of recordings.

#	*Name (date)*	*a_{max} (g)*	*V_{max} (cm/s)*	*M*	*R (km)*	*Comp.*
A	Coyote Lake (8-6-79)	0.321	25.1	5.8	9.6	N320^o
B	Japan-236	0.168	6.1	8.4	185	NS
C	Alkyonides (24-2-81)	0.301	24.4	6.7	32	Trans
D	San Fernando (9-2-71)	0.346	14.5	6.5	23.1	N21^o
E	Coyote Lake (8-6-79)	0.417	43.7	5.8	9.6	N230^o
F	Kalamata (12-9-86)	0.273	23.6	6.2	4	EW
G	San Fernando (9-2-71)	0.278	12.5	6.5	23.1	N291^o
H	Cephalonia (17-1-83)	0.142	8.4	7.0	34	NS
I	Pyrgos (26-3-93)	0.454	19.3	5.5	3	Trans
J	Parkfield (27-6-66)	0.264	14.2	6.1	43.9	N295^o
K	Cephalonia (23-3-83)	0.239	9.8	6.2	13	EW
L	Aigion (15-6-95)	0.543	48.1	6.2	18	N150^o

Observe that site characteristics as well as soil amplification parameters in Table 2 cover a wide range of values, typical for the great majority of potential cases.

The general form of the proposed relations was defined in advance of the statistical analysis of the relevant data, from a joint evaluation of appropriate analytical solutions (e.g. Eq. 3.2) and the trends exhibited by the numerical predictions themselves. Then, a multivariable regression analysis of the entire database, according to the Newton-Raphson iterative procedure, calibrated the 3 to 5 constants of each of the relations. Appropriate weighting was introduced in the statistical analysis to counterbalance the non-uniformity of the database, especially in connection to α^b_{max}, an independent variable with significant influence on all aspects of the response, since it is related to soil non-linearity. In what follows, the results of the equivalent-linear analyses are denoted as data, although they are also simulations and not actual recorded data.

5. PEAK GROUND ACCELERATION

Fig. 3 shows the variation of the relative amplification ratio for the peak ground acceleration, denoted hereafter as A_a, with the normalized soil period T_S/T_e. In this figure, the data are presented in pairs of groups, by maintaining 2 of the remaining free variables fixed within a narrow range, and significantly changing the third variable. Specifically, all data in Fig. 3a correspond to fixed T_b/T_S and n values, but significantly different values of a^b_{max} = 0.01 to 0.14g (moderate shaking) and a^b_{max} = 0.4 to 0.45g (strong shaking). In Fig. 3b, differences in the data correspond to significantly different values of n = 0.5 to 1 (impulse-like motions) and n = 4 to 6 (long duration motions). Finally, in Fig. 3c, the differences correspond to significantly different values of T_b/T_S = 0.05 to 0.4 (high contrast profiles) and T_b/T_S = 0.5 to 0.9 (low contrast profiles).

Observe that the effect of normalized site period T_S/T_e is similar in all figures. Namely, A_a tends to 1.0 as T_S/T_e tends to zero, it becomes maximum close to T_S/T_e=1.0 and it decreases gradually as T_S/T_e exceeds 1.0. This trend is strongly reminiscent of the response of single degree of freedom (SDOF or mass-spring-dashpot) systems subjected to harmonic base excitation. Hence, drawing upon the theory of SDOF vibrations under support excitation (e.g. [2], [13]), the data in Fig. 3 have been fitted by:

$$A_a = \frac{1 + C_{1,a}\left(T_s / T_e\right)^2}{\sqrt{\left[1 - \left(T_s / T_e\right)^2\right]^2 + C_{2,a}^2\left(T_s / T_e\right)^2}} \tag{5.1}$$

According to Eq. (5.1), Aa takes the following characteristic values:

$$A_a = \begin{cases} 1.0 & for\, T_s / T_e = 0 \\ (1 + C_{1,a}) / C_{2,a} & for\, T_s / T_e = 1 \\ C_{1,a} & for\, T_s / T_e \to \infty \end{cases} \tag{5.2}$$

The fact that A_a tends to a fixed, nonzero value at large normalized site periods T_S/T_e is the only basic difference from the response of a SDOF system, which eventually diminishes to zero. This differentiation was conservatively introduced in order to take into account the contribution to the response of the higher modes of vibration.

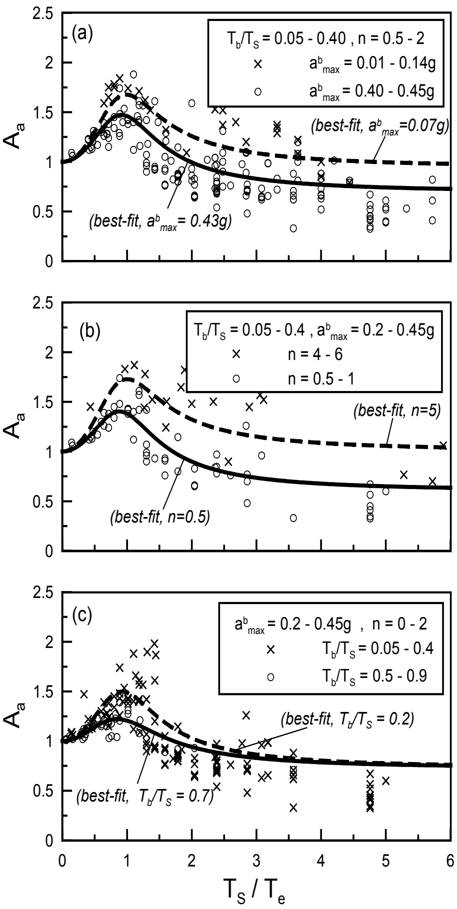

Figure 3: Effect of site and excitation parameters on A_a.
Σχήμα 3: Επίδραση παραμέτρων εδάφους και διέγερσης στο A_a.

In general, the coefficients $C_{1,a}$ and $C_{2,a}$ should be expressed as functions of the three (3) remaining independent variables, i.e. a^b_{max} , T_b/T_S and n. However, the data in Fig. 3 show that $C_{1,a}$, i.e. the asymptotic value of A_a at large normalized soil periods, is not affected by T_b/T_S, but increases consistently as n and a^b_{max} become higher and lower, respectively. Moreover, the value of A_a at resonance increases with increasing n and decreasing a^b_{max}. Hence, $C_{1,a}$ can be expressed as a function of a^b_{max} and n only:

$$C_{1,a} = d_{1,a}\left(\frac{a_{max}}{g}\right)^{d_{2,a}} g(n) \tag{5.3}$$

with

$$g(n) = \frac{n^{d_{3,a}}}{1+n^{d_{3,a}}} \tag{5.4}$$

and $d_{1,a}$(0 , $d_{2,a}$<0 , $d_{3,a}$>0. Note that the general form of g provides an asymptotic increase of $C_{1,a}$ and A_a towards the steady state values, at a large number of cycles n. This effect resembles the transient response of SDOF systems in resonance conditions (e.g. [13]), and is also consistent with the response displayed by the data in Fig. 3b.

Finally, the data in Fig. 3c indicate that the peak value of A_a, tends rather to decrease as the normalized period of the bedrock T_b/T_S becomes higher. This is reasonable since T_b/T_S represents essentially the contrast in dynamic stiffness between the soil and the underlying bedrock, and it is consequently a measure of the radiation damping.

Table 2: Range and Frequency Distribution of Parameters.

Parameter	*Range*	*Distribution*
H (m)	3.5 – 240	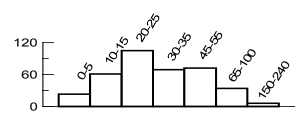
$\overline{V}_{S,o}$ (m/s)	50 – 700	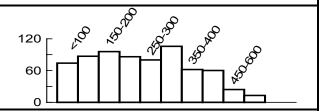
V_b (m/s)	100 – 1000	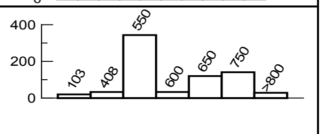
T_S (sec)	0.04 – 3.33	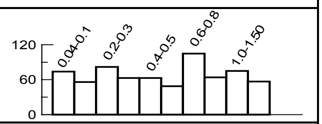
T_b (sec)	0.02 – 1.75	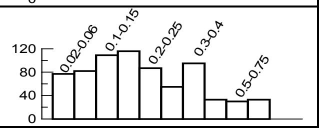
T_b / T_S	0.05 – 0.95	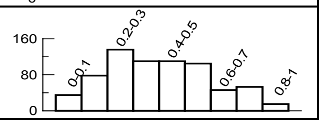
T_S / T_e	0.06 – 13.3	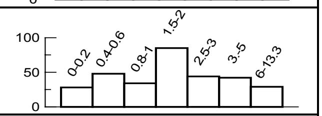
a^b_{max} (g)	0.01 – 0.45	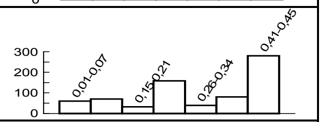
n (cycles)	0.5 – 24	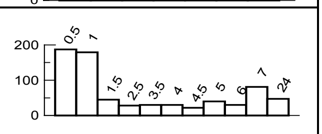

To simulate this effect, $C_{2,a}$ was correlated with T_b/T_S through a linear relation, of the same form as Eq. (3.3), which describes the equivalent critical damping ratio:

$$C_{2,a} = d_{4,a} + d_{5,a} \frac{T_b}{T_S} \tag{5.5}$$

with $d_{4,a}$, $d_{5,a} > 0$.

The constants in Eqs (5.3), (5.4) and (5.5) were determined from a statistical analysis of all available data. This procedure led to a best fit relation for $d_{1,a}$=1.20, $d_{2,a}$= -0.17, $d_{3,a}$=0.50, $d_{4,a}$=1.05 and $d_{5,a}$=0.57. Practically, this *best-fit* relation ensures that A_a is over-predicted in 50% of the cases and under-predicted in the remaining 50% (median value). Note that by changing to $d_{1,a}$=1.75 and retaining the values of the other 4 constants, Eq. (5.1) produces conservative *upper bound* estimates, i.e. ensures overprediction of A_a in 84% of the cases in the database, for added conservatism.

Fig. 4 presents a one-to-one comparison of A_a values, based on the proposed relations (predictions) and the equivalent-linear analyses for all the cases in the database (data). This means that after statistically calibrating Eq. (5.1) for *best fit* and *upper bound* predictions, an a posteriori prediction of A_a for all the cases in the database was performed, as an index of the overall predictive ability of the relation. In addition, Fig. 5 presents another comparison of the *best-fit* predictions and the data, in terms of the relative error R_{Aa}, defined as the difference between approximate predictions of A_a and data normalized with respect to the latter. Observe that the relative error of the *best-fit* relation has practically no bias with respect to the included parameters and that the standard deviation of the error in predicting A_a is +24%. Anyway, some conservative overprediction of A_a is expected for very flexible soil profiles and relatively intense shaking. On the other hand, Fig.4b shows that that the proposed *upper bound* relation provides a consistent overprediction of the whole range of data, and can be used instead of the *best-fit* relation if significant conservatism must be incorporated in the design.

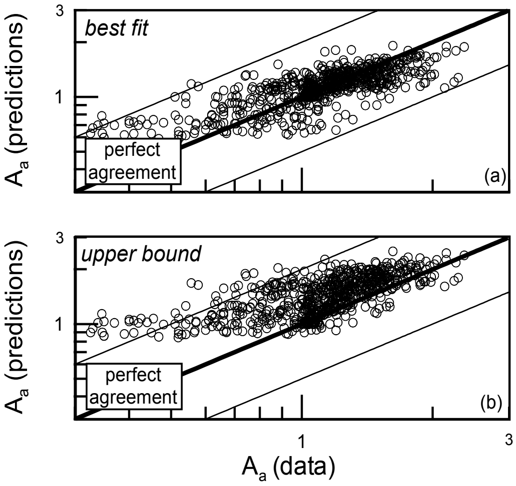

Figure 4: Comparison between predictions and data for Aa.
Σχήμα 4: Σύγκριση προβλέψεων - δεδομένων για το Aa.

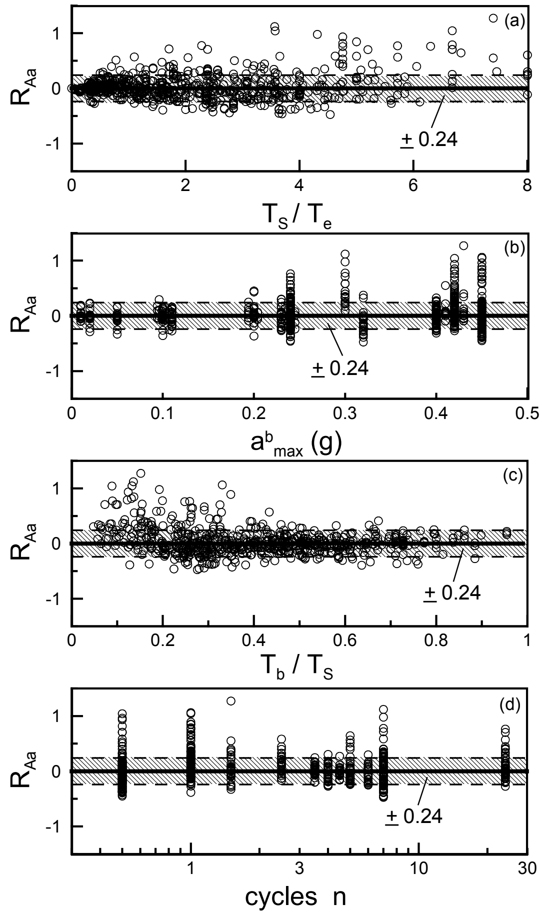

Figure 5: Relative error of proposed relation for A_a.
Σχήμα 5: Σχετικό λάθος της προτεινόμενης σχέσης για το A_a.

6. PEAK GROUND VELOCITY

Numerical predictions for the relative amplification of peak ground velocity A_V, are plotted in Fig. 6 against the normalized soil period T_S/T_e. Specifically, Figs. 6a, 6b and 6c show examples of the effects of the bedrock to soil period ratio T_b/T_S, the peak bedrock acceleration a^b_{max} and the number of equivalent cycles n, respectively. The effect of the various factors on A_V is similar as in the case of A_a, except for two main differences.

The first is that A_V is not consistently affected by the duration of the seismic motion, Fig. 6c. The second difference is that the maximum amplification of the velocity occurs at normalized soil periods T_S/T_e 1. This is because the predominant period of the velocity time history of seismic motions is usually higher than that of the corresponding acceleration time history (e.g. peak spectral velocity usually occurs at larger structural periods than the peak spectral acceleration in tri-logarithmic plots of elastic response spectra).

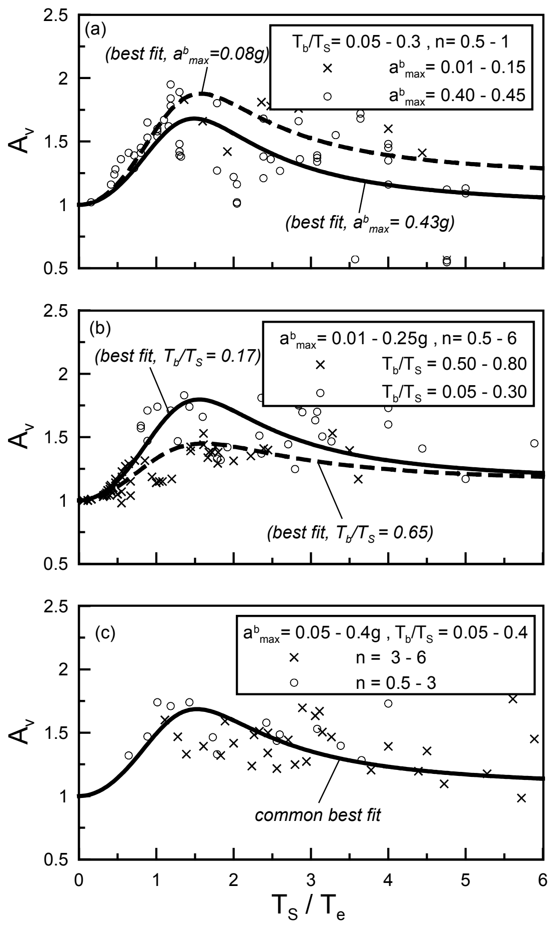

Figure 6: Effect of site and excitation parameters on A_V:.
Σχήμα 6: Επίδραση παραμέτρων εδάφους και διέγερσης στο A_V.

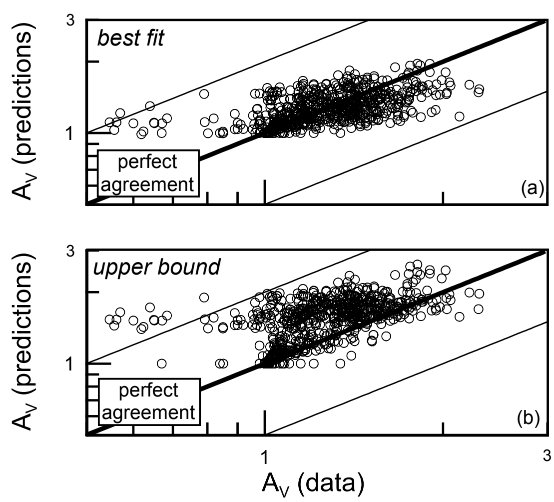

Figure 7: Comparison between predictions and data for AV.
Σχήμα 7: Σύγκριση προβλέψεων - δεδομένων για το AV.

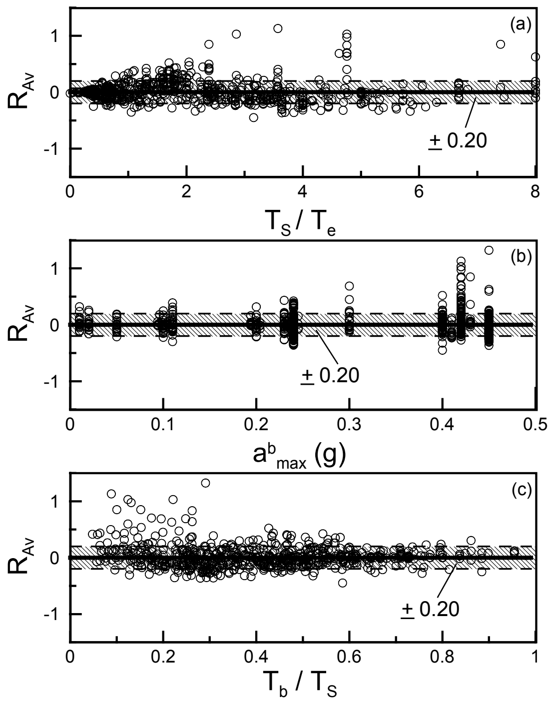

Figure 8: Relative error of proposed relation for A_V.
Σχήμα 8: Σχετικό λάθος της προτεινόμενης σχέσης για το A_V.

According to the data in Fig. 6, the peak amplification occurs at approximately $T_S \cong 1.50\ T_e$. Hence, Eq. (5.1) is re-written as:

$$A_v = \frac{1 + C_{1,v}\left(T_s / 1.5T_e\right)^2}{\sqrt{\left[1 - \left(T_s / 1.5T_e\right)^2\right]^2 + C_{2,v}^2\left(T_s / 1.5T_e\right)^2}} \tag{6.1}$$

where:

$$C_{1,v} = d_{1,v}\left(\frac{a_{max}}{g}\right)^{d_{2,v}} \tag{6.2}$$

$$C_{2,v} = d_{3,v} + d_{4,v}\frac{T_b}{T_s} \tag{6.3}$$

with $d_{2,V}$<0 and $d_{3,V}$, $d_{4,V}$ > 0.

The constants in Eqs (6.2) and (6.3) were again determined from a multi-variable regression analysis of all available data. According to this, the *best fit* relation is obtained for $d_{1,V}$=0.88, $d_{2,V}$=-0.124, $d_{3,V}$=1.087 and $d_{4,V}$=0.598, Practically, this *best-fit* relation provides a median value of A_V, but by changing to $d_{1,V}$=1.25 and retaining the values of the other 3 constants, Eq. (6.1) produces conservative *upper bound* estimates, i.e. ensures overprediction of A_V in 84% of the cases in the database, for added conservatism.

The predictions of A_V are evaluated in Figs. 7. and 8, in the same format as that used to evaluate A_a. In this case, the *best-fit* predictions agree well with the data for A_V >1, with the unbiased relative error R_{Av} having a standard deviation of +19.9%. Anyway, some conservative overprediction of A_V may be expected for very flexible soil profiles, over stiff bedrock and relatively intense seismic excitations, similarly to A_a. Finally, note in Fig. 8b that the proposed *upper bound* fit does provide a consistent overprediction of the whole range of A_V data.

7. FUNDAMENTAL SOIL PERIOD

In order to apply the previous relations in practice, one has to provide the peak acceleration at the outcropping bedrock a^b_{max}, the predominant period of the excitation T_e, as well as the fundamental vibration periods for the bedrock T_b and for the soil T_S. Among these parameters, a^b_{max} and T_e are usually provided by a seismic hazard study while T_b is related by definition to the soil thickness H and the elastic shear wave velocity of the bedrock V_b (i.e. T_b=4H/V_b). In contrast, estimation of T_S is not equally straightforward, even if the variation of elastic shear wave velocity with depth is known. This is mostly due to the fact that soil response during shaking is non-linear and consequently the fundamental period T_S is related to the applied shear stresses and strains in addition to the elastic soil properties. Fig. 9 shows typical experimental curves for the variation of the shear modulus G, normalized against the elastic shear modulus G_o, with applied cyclic shear strain amplitude γ, for soils with different plasticity index I_p [25]. Analytically, these curves are approximately expressed as:

$$\frac{G}{G_o} = \frac{1}{1+\kappa\gamma^{\lambda}} \tag{7.1}$$

For instance, Eq. (7.1) with κ=6, λ=0.91 and γ in (%) is compared to the experimental curve for I_p =30% in Fig. 9. In terms of shear wave velocities, Eq. (7.1) becomes:

$$\left(\frac{V_S}{V_{S,o}}\right)^2 = \frac{1}{1+\kappa\gamma^{\lambda}} \tag{7.2}$$

where V_S denotes the shear wave velocity for cyclic shear strain amplitude γ, while $V_{S,o}$ denotes its value for $\gamma < 10^{-5}$. Based on Eq. (7.2), a general relation for the fundamental soil period T_S is:

$$\left(\frac{T_S}{T_{S,o}}\right)^2 = 1+\kappa\gamma^{\lambda} \tag{7.3}$$

where $T_{S,o}$ denotes the elastic soil period (for $\gamma < 10^{-5}$).

As a first approximation, the γ may be related to a^b_{max}, as an index of the shaking intensity, and the average elastic shear wave velocity $V_{S,o}$ (=4H/$T_{S,o}$), as an index of the dynamic soil stiffness. Hence, Eq. (7.3) is written as:

$$\left(\frac{T_S}{T_{S,o}}\right)^2 = 1 + d_{1,T}\left(\bar{V}_{s,o}\right)^{d_{2,T}}\left(\frac{\alpha^b{}_{\max}}{g}\right)^{d_{3,T}} \tag{7.4}$$

with $d_{1,T}$, $d_{3,T}$ > 0 and $d_{2,T}$ < 0.

The values of these constants were estimated from a multi-variable regression analysis, as: $d_{1,T}$ = 5330, $d_{2,T}$ = -1.30 and $d_{3,T}$ = 1.04.

Fig. 10 presents a one-to-one comparison between T_S predictions and results from the analyses (data). Fig. 11 provides the relative error R_{Ts} as a function of the two basic input parameters a^b_{max} and $V_{S,o}$ It is argued that Eq. (7.4) follows closely the trends of the data, in qualitative and quantitative terms (standard deviation +24.3%).

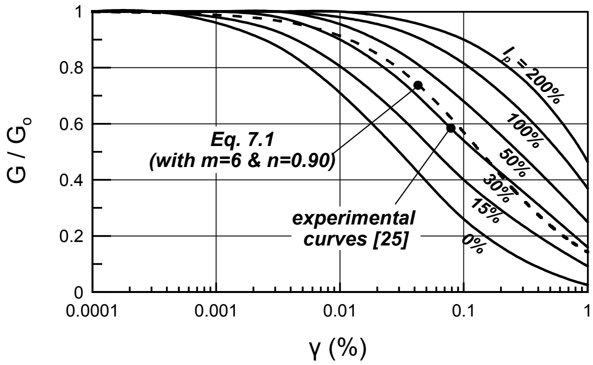

Figure 9: Variation of G with shear strain γ.
Σχήμα 9: Μεταβολή του G με την διατμητική παραμόρφωση γ.

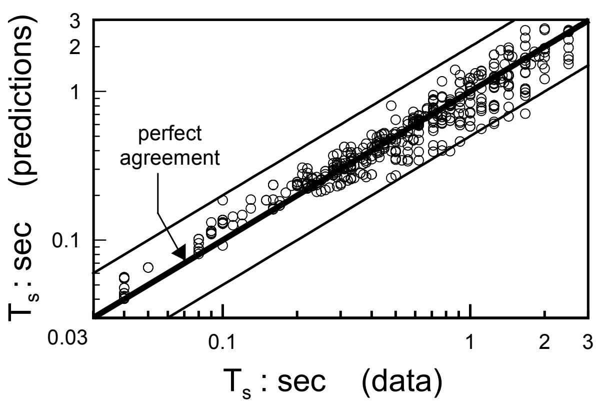

Figure 10: Comparison between predictions and data for TS.
Σχήμα 10: Σύγκριση προβλέψεων - δεδομένων για το TS.

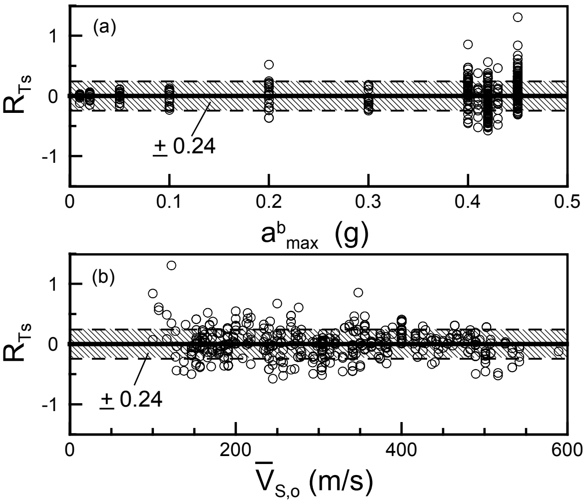

Figure 11: Relative error of proposed relation for T_S.
Σχήμα 11: Σχετικό λάθος της προτεινόμενης σχέσης για το T_S.

8. DISCUSSION

The proposed relations estimate soil effects on peak ground acceleration and velocity in terms of four (4) basic parameters: period ratios T_S/T_e and T_b/T_S, α^b_{max} and n. These four parameters are treated as independent, given that their covariance coefficient is in all cases smaller than 0.15 (note that a covariance coefficient equal to 1.0 corresponds to total dependence between two variables). According to the statistical analysis, the effect of T_S/T_e is the most systematic and pronounced, at least for low values of T_b/T_S (< 0.40). The effects of the remaining parameters are relatively less significant.

The effect of soil non-linearity on T_S is estimated as a function of two (2) obviously independent variables: the average small-strain shear wave velocity $V_{S,o}$ of the soil, and a^b_{max}. In this case, the statistical analysis indicates that the importance of these variables is broadly equivalent.

In addition to the evaluation of the proposed relations against the numerical predictions used in the statistical analysis, their accuracy was verified in a series of case studies (not included in the database): a) two (2) sites in the San Fernando Valley during the *Northridge* earthquake (January 17th 1994), and b) five (5) seismic events recorded by the *SMART-1* accelerometer array in Taiwan. Full details of the site characteristics (e.g. geology, V_S profile with depth) and the recordings (i.e. earthquake magnitude, elastic response spectra) for these case studies are provided in [5]. In this paper, the information regarding the site characteristics and the recordings for the seven (7) case studies is outlined in Table 3, in the processed form of the parameters entering the proposed relations. Observe that the sites and the seismic events considered cover a wide range of potential cases, rendering this evaluation representative for a wide range of applications in practice.

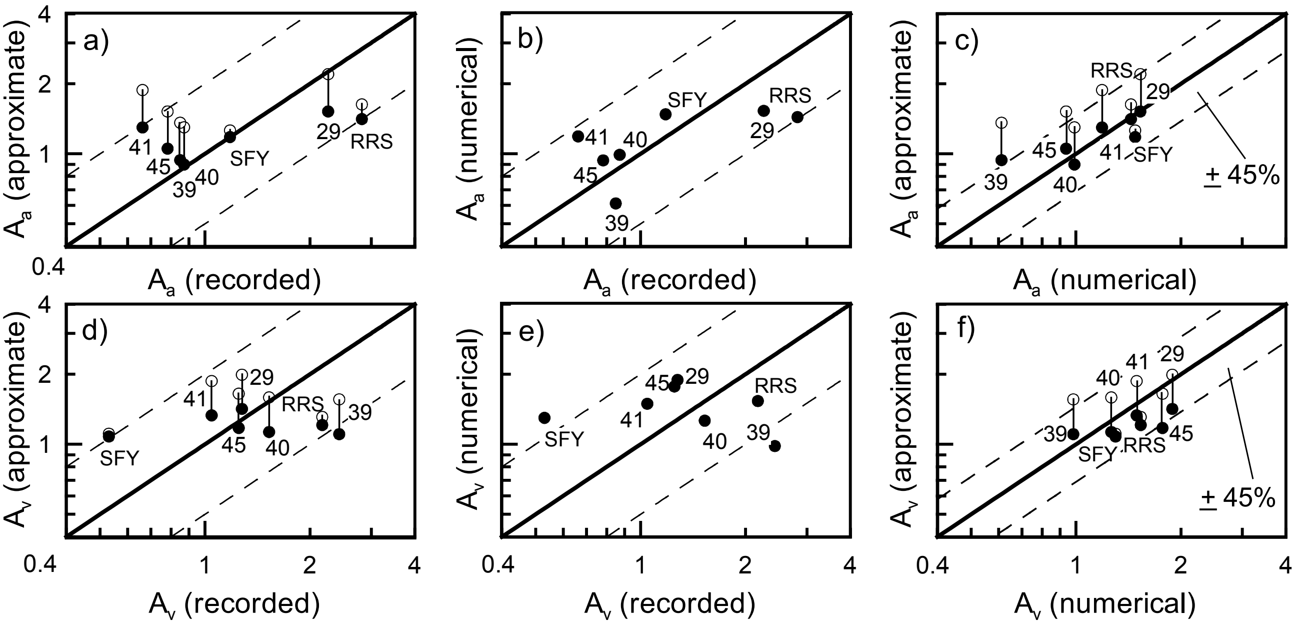

Figure 12: Evaluation of best fit (() and upper bound (o) relations against seismic recordings and numerical predictions; (a), (b) & (c) for Aa; (d), (e) & (f) for AV.
Σχήμα 12: Αποτίμηση βέλτιστων σχέσεων (() και σχέσεων άνω ορίου (o) έναντι σεισμικών καταγραφών και αριθμητικών προβλέψεων: (a), (b) & (c) για το Αα - (d), (e) & (f) για το AV.

Table 3: Outline of site and seismic excitation input parameters for the verification case studies

#	a^b_{max} (g)	T_e (sec)	n	$T_{s,o}$ (sec)	$\overline{V}_{S,o}$ (m/s)	T_b (sec)
29	0.033	0.22	5	1.13	283	0.58
39	0.200	0.16	2	1.13	283	0.58
40	0.190	0.20	1.5	1.13	283	0.58
41	0.050	0.19	3	1.13	283	0.58
45	0.140	0.20	2.5	1.13	283	0.58
RRS	0.291	1.00	4	0.59	494	0.37
SFY	0.291	1.00	4	0.33	408	0.21

For each one of the seven (7) case studies, soil amplification was estimated by three methods: a) direct calculation from the actual *recorded* time-histories in the surface of nearby 'soil' and the 'bedrock' sites, b) *approximate* calculations via the best fit proposed relations, and c) *numerical* calculations with the equivalent-linear method [14]. The three sets of data are compared to each other in Fig. 12 (solid circles). Observe first that the approximate relations estimate the recorded A_a and A_V with a safety factor equal to 2 and no systematic bias (Figs 12a and 12d). Note also that the same lever of accuracy is obtained from the simulations with the equivalent-linear method (Figs 12b & 12e). This is clearly an indication of the widely acknowledged difficulties encountered when field data are interpreted on the basis of theoretical models. Finally, note in Figs 12c & 12f that the approximate best fit predictions fall consistently within ±45% of their numerical counterparts, without any systematic bias. On the other hand, the comparisons for approximate *upper bound* predictions in the same figure (hollow circles) show that these consistently overpredict numerical and recorded data, ensuring a reasonable level of conservatism.

9. CONCLUSIONS

A set of approximate relations has been established to evaluate soil effects on a_{max} and V_{max}, and also to estimate the basic site parameter, i.e. the non-linear soil period T_S. The basic parameters of the relations are identified through a simplified analytical simulation of the problem. Their effect is quantified via a statistical analysis of data obtained from over 700 equivalent-linear analyses of seismic ground response and not from seismic recordings. In summary, it was found that:

a) Soil effects on a_{max} are a function of the period ratios T_S/T_e and T_b/T_S, the peak bedrock acceleration a^b_{max} and the equivalent number of cycles *n*. Soil effects on V_{max} depend on the same parameters, except for n.

b) The non-linear soil period T_S is related with the elastic soil period $T_{S,o}$, the average elastic shear wave velocity $V_{S,o}$ over the entire soil depth, and a^b_{max}.

c) Predictions obtained from the proposed *best-fit* relations are usually within ± 19.9 to 24.3% from the respective estimates from equivalent-linear analyses. On the other hand, the upper bound relations provide consistently conservative upper bound estimates of the numerical results.

d) Evaluation of the proposed relations in well-documented cases of actual recordings and numerical analyses that are not included in the database verified the above safety margins.

Nevertheless, the accuracy of the proposed relations is conceptually related to, and limited by, the accuracy of the equivalent-linear method ([14], [22]) used to obtain the numerical predictions in the database. Furthermore, their application should be limited to cases where the site and excitation characteristics fall within the limits summarized in Table 2. Further details concerning the relations and their verification can be found in [4]. Overall, the relations should be considered as approximate, aimed at the preliminary evaluation of soil effects. In addition, they can be used as a user-friendly alternative to the equivalent-linear method, when the latter is too cumbersome to implement, as in GIS-aided microzonation studies [21].

10. ACKNOWLEDGEMENTS

This research was funded by the Earthquake Protection and Planning Organization of Greece (Ο.Α.Σ.Π.). Professor G. Gazetas has contributed valuable comments on the paper presentation, while fellow Civil Engineers Thomas Panourgias, Michael Klouvas and Niki Kringos assisted with the statistical analysis and the verification of the relations. These contributions are gratefully acknowledged.

11. APPENDIX

Analysis of soil effects for harmonic excitation and uniform visco-elastic soil and bedrock conditions

Based on one-dimensional wave propagation theory, the amplification of the seismic excitation from the outcropping bedrock to the free soil surface, in the simplified case of a uniform soil and bedrock site, is expressed as (e.g. [16]):

$$A_{s,o} = \frac{1}{cos\, k_s^* H + i\alpha^*\ sin\, k_s^* H} \tag{I.1}$$

where

$$k_s^* H = \frac{\omega H}{V_s^*}\ ,\ V_s^* = V_s(1 + i\xi_s)\ ,\ \alpha^* = \alpha \frac{1 + i\xi_s}{1 + i\xi_b}\ ,$$

and

$$\alpha = \frac{\rho_s}{\rho_b}\frac{T_b}{T_s}$$

Taking into account that for small values of ξ_s (i.e. $\xi s < 0.10$): $k_s^* H \approx k_s H(1 - i\xi_s)$ and that by definition cos(ix)= cosh(x) and sin(ix)= i sinh(x), the complex trigonometric terms in Eq. (I.1) are written as:

$$cos(k_s^* H) \approx cos\left[k_s H\left(1 - i\xi_s\right)\right] = \\ = cos(k_s H)\,cosh(\xi_s k_s H) + i\,sin(k_s H)\,sinh(\xi_s k_s H) \tag{I.2}$$

and:

$$sin(k_s^* H) \approx sin\left[k_s H\left(1 - i\xi_s\right)\right] = \\ = sin(k_s H)\,cosh(\xi_s k_s H) - i\,cos(k_s H)\,sinh(\xi_s k_s H) \tag{I.3}$$

Furthermore, for small values of ξs,

$$\alpha^* = \alpha\frac{1 + i\xi_s}{1 + i\xi_b} \approx \alpha\left[1 + i(\xi_s - \xi_b)\right] \tag{I.4}$$

Hence, Eq. (I.1) is expanded as shown below (Eq. I.5):

$$\frac{1}{A_{s,o}} = \cos(k_s H)\cosh(\xi_s k_s H) + \alpha\cos(k_s H)\sinh(\xi_s k_s H) \\ - \alpha(\xi_s - \xi_b)\sin(k_s H)\cosh(\xi_s k_s H) \\ + i\begin{bmatrix} sin(k_s H)\,sinh(\xi_s k_s H) + \alpha\,sin(k_s H)\,cosh(\xi_s k_s H) + \\ \alpha(\xi_s - \xi_r)\,cos(k_s H)\,sinh(\xi_s k_s H) \end{bmatrix}$$

and consequently (Eq. I.6):

$$\left|\frac{1}{A_{s,o}}\right|^2 = cos^2(k_s H) + sinh^2(\xi_s k_s H) + \\ \alpha^2\left[sin^2(k_s H) + sinh^2(\xi_s k_s H)\right]\left[1 + (\xi_s - \xi_b)^2\right] \\ + 2\alpha\begin{bmatrix} cosh(\xi_s k_s H)\,sinh(\xi_s k_s H) - \\ (\xi_s - \xi_b)\,cos(k_s H)\,sin(k_s H) \end{bmatrix}$$

For the special case where the bedrock and the soil have the same properties (i.e. a=1, $\xi s = \xi b$), Eq. (I.6) simplifies to:

$$\left|\frac{1}{A_{b,o}}\right| = cosh(\xi_b k_b H) + sinh(\xi_b k_b H) = exp(\xi_b k_b H) \tag{I.7}$$

Furthermore, for low values of ξs and ξb, as well as high contrast between the shear wave velocities of the bedrock and the soil (i.e. low a values), Eq. (I.6) may be written as:

$$\left|A_{s,o}\right| = \frac{1}{\sqrt{cos^2\left(k_s H\right) + \left[\xi_{e,s}\left(k_s H\right)\right]^2}} \tag{I.8}$$

or, introducing the excitation period $Te = 2\pi/\omega$ and the predominant soil period $TS = 4H/V_S$:

$$\left|A_{s,o}\right| = \frac{1}{\sqrt{cos^2\left(\frac{\pi}{2}\frac{T_s}{T_e}\right) + \left[\xi_{e,s}\left(\frac{\pi}{2}\frac{T_s}{T_e}\right)\right]^2}} \tag{I.9}$$

where:

$$\xi_{e,s} = \xi_s + \frac{2}{\pi}\alpha\frac{T_e}{T_s}$$

Eqs. (I.7) and (I.9) provide the amplification ratios for seismic waves propagating vertically within the seismic bedrock and within the soil. Hence, the relative amplification ratio, from the free surface of the seismic bedrock to that of the soil is given in complex function form as:

$$\left|A_s\right| = \frac{exp\left[\left(\xi_b\frac{T_b}{T_s}\right)\frac{\pi}{2}\frac{T_s}{T_e}\right]}{\left|cos\left(\frac{\pi}{2}\frac{T_s^*}{T_e}\right) + i\alpha^*\,sin\left(\frac{\pi}{2}\frac{T_s^*}{T_e}\right)\right|} \tag{I.10}$$

or, approximately:

$$\left|A_s\right| = \frac{exp\left[\left(\xi_b\frac{T_b}{T_s}\right)\frac{\pi}{2}\frac{T_s}{T_e}\right]}{\sqrt{cos^2\left(\frac{\pi}{2}\frac{T_s}{T_e}\right) + \left[\xi_{e,s}\left(\frac{\pi}{2}\frac{T_s}{T_e}\right)\right]^2}} \tag{I.11}$$

12. REFERENCES

1. Ambraseys N. N., Simpson K.A., Bommer J. J. (1996), "Prediction of horizontal response spectra in Europe", **Earthquake Engineering and Structural Dynamics, Vol. 25**, pp. 371-400.

2. Biggs J. M. (1965), **"Introduction to structural dynamics"**, McGraw-Hill, p. 341.

3. Bouckovalas G. (1997), "Prediction of Soil effects on Seismic Motions: A comparative Case Study", **Earthquake Spectra, Vol. 13**, No. 3, August.

4. Bouckovalas G. D., Papadimitriou A. G. (2003), "Multi-variable relations for soil effects on seismic ground motion", **Earthquake Engineering and Structural Dynamics, Vol.32**, No.12, 1867-1896.

5. Bouckovalas G. D., Papadimitriou A. G. (2004) "Multi-variable relations for soil effects on elastic response spectra", **Technika Chronika**.

6. Boore D. M., Joyner W. D., Fumal T. E. (1993), "Estimation of response spectra and peak accelerations from Western North America earthquakes: An interim report", **U.S.G.S., Open File Report 93-509**, p. 72.

7. Boore D. M., Joyner W. D., Fumal T. E. (1994), "Estimation of response spectra and peak accelerations from Western North America earthquakes: An interim report (Part 2)", **U.S.G.S., Open File Report 94-127**, p. 40.

8. Boore D. M., Joyner W.D., Fumal T. E. (1997), "Empirical near-source attenuation relationships for horizontal and vertical peak ground acceleration, peak ground velocity and pseudo-absolute acceleration response spectra", **Seismological Research Letters, Vol. 168**, No. 1, pp. 154-179.

9. Borchert R. D. (1991), "Estimates for site dependent response

spectra for design (methodology and justification)", **Earthquake Spectra, 10**, No.4, 617-653.

10. Borja R. I., Chao H. Y., Montans F. J., Lin C. H. (1999), "Non-linear ground response at Lotung LSST site", **Journal of Geotechnical and Geoenvironmental Engineering, ASCE, Vol. 120**, No.3, 491-513.

11. Chang C.-Y., Mok C. M., Power M. S. (1991), "Analysis of ground response data from Lotung large scale soil-structure interaction experiment site", **Report NP-7306-SL, Electric Power Research Institute**, Palo Alto, California.

12. Chen C.-H., Chiu H. C. (1999), "Identification of shear wave velocity from earthquake ground motions", Proceedings, **2nd International Conference on Earthquake Geotechnical Engineering**, Lisbon, June 21-25, pp. 205 – 210.

13. Chopra A. K. (1995), **"Dynamics of structures: theory and applications to earthquake engineering"**, Prentice Hall, p. 729.

14. Idriss I. M., Sun J. I. (1992), "SHAKE91 – A computer program for conducting equivalent linear seismic response analysis of horizontally layered soil deposits", **User's Guide**, Center for Geotechnical Modeling, Civil Engineering Department, U.C. Davis.

15. Kawashima K., Aizawa K., Takashi K. (1986), "Attenuation of peak ground acceleration, velocity and displacement based upon multiple regression of Japanese strong ground motion records", **Earthquake Engineering and Structural Dynamics, 14**: 481 – 490.

16. Kramer S. L. (1996), **"Geotechnical Earthquake Engineering"**, Prentice Hall, p. 653.

17. Lee M., Finn L. (1978), "Program for the Dynamic Effective Stress Response Analysis of soil deposits including liquefaction evaluation", **Research Report, University of British Columbia**, Faculty of Applied Sciences, June.

18. Mellal A., Modaressi H. (1998), "A simplified numerical approach for nonlinear dynamic analysis of multi-layered media", Proceedings, **11th European Conference on Earthquake Engineering**, Paris, September 6 – 11.

19. Midorikawa S., Matsuoka M., Sakugawa K. (1994), "Site effects on strong motion records observed during the 1987 Chiba-ken-toho-oki, Japan earthquake", Proceedings, **9th Japan Earthquake Engineering Symposium**, December, Tokyo, 3: 85 – 90.

20. Mok C. M., Chang C.-Y., Legaspi D. E. (1998), "Site response analyses of vertical excitation", Proceedings, **Geotechnical Earthquake Engineering and Soil Dynamics III**, ASCE, Seattle, Washington, August 3 – 6.

21. Papadimitriou A. G., Antoniou A., Bouckovalas G. D., Marinos P. (2004), "Approximate relations for GIS-aided evaluation of soil effects on seismic ground motion", Proceedings, **11th IC Soil Dynamics Earthquake Engineering & 3rd IC Earthquake Geotechnical Engineering**, Vol.2, 39-46, Berkeley, USA, January.

22. Schnabel P. B., Lysmer J., Seed H. B. (1972), "SHAKE – A computer program for earthquake response analyses of layered soils", **User's manual**, EERC – 72, Berkeley, CA.

23. Soeda Y., Tamai H., Nakatsu N. (1999), "Nonlinearity and irregularity of strong seismic motions by vertical arrays during the 1995 Kobe earthquake", Proceedings, **2nd International Conference on Earthquake Geotechnical Engineering**, Lisbon, June 21 – 25, pp. 225 – 230.

24. Spudich P., Joyner W.B., Lindh A.G., Boore D.M., Margaris B.M., Fletcher J.B. (1999), "SEA99 - A revised ground motion prediction relation for use in extensional tectonic regimes", **Bulletin Seismological Society America, Vol. 89**, No. 5, pp. 1156-1170.

25. Vucetic M., Dobry R. (1991), "Effect of soil plasticity on cyclic response", **Journal of Geotechnical Engineering Division, ASCE, Vol. 120**, No.12, pp 2208 – 2228.

George D. Bouckovalas
Professor, Geotechnical Department, School of Civil Engineering, National Technical University of Athens.
Achilleas G. Papadimitriou
Dr Civil Engineer, Geotechnical Department, School of Civil Engineering, National Technical University of Athens.

Εκτενής περίληψη

Παραμετρικές Σχέσεις Υπολογισμού της Εδαφικής Ενίσχυσης Ι. Μέγιστη Σεισμική Επιτάχυνση και Ταχύτητα

ΓΕΩΡΓΙΟΣ Δ. ΜΠΟΥΚΟΒΑΛΑΣ
Καθηγητής Ε.Μ.Π.

ΑΧΙΛΛΕΑΣ Γ. ΠΑΠΑΔΗΜΗΤΡΙΟΥ
Δρ Πολιτικός Μηχανικός Ε.Μ.Π.

Περίληψη

Η επίδραση του εδάφους στη μέγιστη σεισμική επιτάχυνση και ταχύτητα εκφράζεται μέσω απλών σχέσεων υπολογισμού, ως συνάρτηση πέντε (5) βασικών παραμέτρων του εδάφους και της διέγερσης: των ιδιοπεριόδων του εδάφους T_S και του υποβάθρου T_b, της δεσπόζουσας περιόδου της διέγερσης T_e, της μέγιστης σεισμικής επιτάχυνσης στο αναδυόμενο υπόβαθρο a^b_{max} και του αριθμού ισοδύναμων κύκλων n. Επιπλέον, προτείνεται και μία σχέση για τον υπολογισμό της T_S ως συνάρτηση του πάχους της εδαφικής στήλης H, της μέσης ταχύτητας διατμητικών κυμάτων στο έδαφος $V_{S,o}$ και της a^b_{max}. Όλες αυτές οι σχέσεις διατυπώθηκαν ακολουθώντας δύο βήματα: (α) οι βασικές παράμετροι αναγνωρίσθηκαν μέσω αναλυτικής προσομοίωσης της εδαφικής απόκρισης υπό αρμονική διέγερση και (β) η επίδραση της κάθε παραμέτρου εκτιμήθηκε μέσω στατιστικής ανάλυσης σχετικών δεδομένων από πλέον των 700 μονοδιάστατων ισοδύναμα γραμμικών αναλύσεων σεισμικής απόκρισης. Στις αριθμητικές αναλύσεις χρησιμοποιήθηκαν εδαφικά προφίλ που αντιστοιχούν σε πραγματικές θέσεις και σεισμικές διεγέρσεις που προέρχονται από πραγματικές καταγραφές σεισμών. Η σύγκριση με επτά (7) πραγματικές καταγραφές εδαφικής επίδρασης δείχνει ότι η ακρίβεια των προτεινόμενων σχέσεων είναι συγκρίσιμη με αυτή της ισοδύναμα γραμμικής μεθόδου. Συνεπώς, οι εν λόγω σχέσεις μπορούν να χρησιμοποιηθούν ως μία εύχρηστη εναλλακτική της είτε για προκαταρκτικές μελέτες είτε για μελέτες με χρήση λογιστικών φύλλων (π.χ. μικροζωνικές μελέτες με χρήση GIS) όπου η ενσωμάτωση αριθμητικών μεθόδων είναι δύσκολη.

Είναι σήμερα ευρέως αποδεκτό ότι το έδαφος διαφοροποιεί τα χαρακτηριστικά των σεισμικών κυμάτων έτσι, ώστε τόσο η ένταση όσο και τα φασματικά χαρακτηριστικά της σεισμικής δόνησης στην ελεύθερη επιφάνεια παρακείμενων εδαφικών και βραχωδών σχηματισμών να διαφέρουν. Το φαινόμενο αυτό είναι γνωστό ως «*εδαφική ενίσχυση*», αν και δεν οδηγεί πάντοτε σε ενίσχυση της δόνησης. Αντίστοιχες βέβαια μπορεί να είναι και οι επιδράσεις της τοπογραφίας του εδάφους και της γεωμετρίας του υποβάθρου σε μία θέση, αλλά η ανάλυσή τους κατά τον αντισεισμικό σχεδιασμό τεχνικών έργων έπεται συνήθως της ανάλυσης της εδαφικής ενίσχυσης.

Υποβλήθηκε: 30.10.2002 Έγινε δεκτή: 1.7.2004

Οι μέθοδοι ποσοτικής αποτίμησης της εδαφικής ενίσχυσης διαχωρίζονται σε:

e) *Εμπειρικές*, οι οποίες συσχετίζουν τις εδαφικές συνθήκες με τα χαρακτηριστικά της σεισμικής δόνησης, και έχουν προέλθει από στατιστική επεξεργασία πραγματικών σεισμικών καταγραφών (π.χ. [1], [6], [7], [8], [9], [15], [19], [24]).

f) *Αριθμητικές*, οι οποίες προσομοιώνουν τη μονοδιάστατη μετάδοση σεισμικών κυμάτων, από το σεισμικό υπόβαθρο στην ελεύθερη επιφάνεια του εδάφους και αντίστροφα, με τη μέθοδο των Πεπερασμένων Στοιχείων ή των Πεπερασμένων Διαφορών (π.χ. [14], [17], [18], [22]).

Οι *εμπειρικές μέθοδοι* είναι συνήθως μονο-παραμετρικές και έτσι η εφαρμογή τους είναι άμεση και απλή. Όπως είναι όμως φυσικό, δεν μπορούν να λάβουν υπόψη όλες τις πτυχές της αλληλεπίδρασης εδαφικής στήλης - διέγερσης (π.χ. συντονισμός ή επίδραση στρωματογραφίας εδάφους), με συνέπεια να προσφέρουν μειωμένη ακρίβεια, ιδιαίτερα σε σχέση με τον αντισεισμικό σχεδιασμό τεχνικών έργων [3]. Οι *αριθμητικές μέθοδοι* είναι απαλλαγμένες από τους ανωτέρω περιορισμούς, αλλά η εφαρμογή τους σε συνήθη τεχνικά έργα προσκόπτει συνήθως στο χρόνο και το κόστος που απαιτείται για τη λεπτομερή αποτίμηση των εδαφικών παραμέτρων και την εκτέλεση των αναλύσεων.

Οι σχέσεις, που προτείνονται εδώ, είναι πολυπαραμετρικές και αναπτύχθηκαν, προκειμένου να γεφυρωθεί το κενό μεταξύ εμπειρικών και αριθμητικών μεθόδων. Με την εισαγωγή περισσότερων γεωτεχνικών και σεισμολογικών παραμέτρων οι προτεινόμενες σχέσεις περιγράφουν πλέον με μεγαλύτερη λεπτομέρεια το φαινόμενο της εδαφικής ενίσχυσης, ενώ διατηρούν το πλεονέκτημα της άμεσης και απλής εφαρμογής. Ιδιαίτερης σημασίας θεωρείται το γεγονός ότι, σε αντίθεση με τις αριθμητικές μεθόδους, μπορούν εύκολα να ενσωματωθούν σε Γεωγραφικά Συστήματα Πληροφοριών (G.I.S.), και έτσι να συμβάλουν στην αυτοματοποίηση των *Μικροζωνικών Μελετών* σεισμικής επικινδυνότητας αστικών περιοχών [21] ή εκτεταμένων έργων υποδομής (π.χ.

συστήματα αγωγών, οδικά δίκτυα κ.λπ.).

Η πρωτοτυπία στη διατύπωση των νέων σχέσεων έγκειται σε δύο κυρίως σημεία. Κατά πρώτον, η επιλογή των γεωτεχνικών - σεισμολογικών παραμέτρων έγινε με βάση αναλυτικές λύσεις κυματικής διάδοσης για ομοιόμορφα ιξωδοελαστικά εδάφη και αρμονικές σεισμικές διεγέρσεις. Κατά δεύτερον, η διατύπωση των σχέσεων έγινε μετά από στατιστική επεξεργασία αποτελεσμάτων πλέον των 700 αριθμητικών αναλύσεων σεισμικής απόκρισης του εδάφους, για πραγματικές σεισμικές διεγέρσεις και φυσικά εδάφη, τις οποίες έχουν εκτελέσει οι συγγραφείς στο πλαίσιο τεχνικών μελετών και ερευνητικών προγραμμάτων. Όλες οι αριθμητικές αναλύσεις έγιναν σύμφωνα με την *ισοδύναμη-γραμμική* μέθοδο, η οποία είναι η συνηθέστερα χρησιμοποιούμενη κατά την τελευταία 30-ετία, δηλαδή με τα λογισμικά SHAKE [22] και κυρίως το SHAKE91 [14]. Αντίστοιχη στατιστική επεξεργασία σεισμολογικών δεδομένων δεν είναι επί του παρόντος εφικτή, δεδομένου ότι μικρό μόνον ποσοστό των διαθέσιμων σεισμικών καταγραφών έχουν γίνει σε θέσεις με γνωστά γεωτεχνικά χαρακτηριστικά.

Το παρόν άρθρο αναφέρεται στις σχέσεις εδαφικής ενίσχυσης για τη μέγιστη σεισμική επιτάχυνση a_{max} και ταχύτητα V_{max} και στον υπολογισμό της ιδιοπεριόδου της εδαφικής στήλης T_S, ενώ το συνοδό άρθρο [5] αναφέρεται σε ανάλογες σχέσεις για τα ελαστικά φάσματα απόκρισης. Συγκεκριμένα, για τη συσχέτιση των a_{max} και V_{max} στην ελεύθερη επιφάνεια του εδάφους και του παρακείμενου βραχώδους υποβάθρου ορίζονται δύο συντελεστές εδαφικής ενίσχυσης A_a και A_V (Εξισώσεις 5.1 και 6.1) συναρτήσει των εξής βασικών παραμέτρων του εδάφους και της διέγερσης, δηλαδή:

(α) του λόγου της ιδιοπεριόδου της εδαφικής στήλης προς τη δεσπόζουσα περίοδο της διέγερσης T_S/T_e ,
(β) του λόγου ιδιοπεριόδων της στήλης εδάφους και ίσου ύψους στήλης βραχώδους υποβάθρου T_S/T_b,
(γ) της μέγιστης σεισμικής επιτάχυνσης στην ελεύθερη επιφάνεια του βραχώδους υποβάθρου α^b_{max}, και
(δ) του αριθμού των ισοδύναμων αρμονικών κύκλων της διέγερσης n.

Η ιδιοπερίοδος T_S εκφράζεται ως συνάρτηση της αντίστοιχης γραμμικής ιδιοπεριόδου $T_{S,o}$ και δύο ανεξαρτήτων παραμέτρων (Εξίσωση 7.4):

(α) της μέσης ταχύτητας μετάδοσης σεισμικών (διατμητικών) κυμάτων στο έδαφος $V_{S,o}$ και
(β) της μέγιστης σεισμικής επιτάχυνσης στην ελεύθερη επιφάνεια του βραχώδους υποβάθρου α^b_{max}.

Για τους συντελεστές εδαφικής ενίσχυσης A_a και A_V, η παράμετρος T_S/T_e αναδεικνύεται ως η πλέον βαρύνουσα, τουλάχιστον για έντονες διαφορές δυσκαμψίας εδάφους και βραχώδους υποβάθρου (T_b/T_S < 0.40), χωρίς όμως να μπορεί να αμεληθεί η συμβολή καμιάς από τις υπόλοιπες τρεις παραμέτρους. Αντίθετα, για την ιδιοπερίοδο της εδαφικής στήλης T_S , και οι δύο παράμετροι, που υπεισέρχονται στη σχέση έχουν την ίδια βαρύτητα.

Αρχικά, οι προτεινόμενες σχέσεις αξιολογήθηκαν σε σύγκριση με τα αποτελέσματα των αριθμητικών αναλύσεων που χρησιμοποιήθηκαν για τη στατιστική επεξεργασία (Σχήματα 4, 5, 7, 8, 10 και 11). Από τη σύγκριση αυτή προκύπτει ότι η απόκλιση των προσεγγιστικών από τις αριθμητικές εκτιμήσεις δεν παρουσιάζει μεγάλη διασπορά (τυπική απόκλιση του λάθους + 20 - 24%), μα το πιο σημαντικό είναι ότι η όποια απόκλιση είναι πρακτικώς τυχαία, δηλαδή δεν συσχετίζεται με κάποια από τις ανεξάρτητες παραμέτρους. Ακολούθως, έγινε και σύγκριση με πραγματικά σεισμολογικά δεδομένα από επτά (7) καλά τεκμηριωμένες περιπτώσεις εδαφικής ενίσχυσης: δύο (2) από την κοιλάδα San Fernando κατά το σεισμό του Northridge (Ιαν. 1994) και άλλες πέντε (5) από το σεισμολογικό δίκτυο SMART-1 της Taiwan. Λεπτομερής παρουσίαση των ιστορικών περιστατικών παρουσιάζεται στο συνοδό άρθρο [5]. Στο παρόν άρθρο εμφανίζεται μόνον η σύγκριση των προσεγγιστικών εκτιμήσεων των A_a και A_V με τις αντίστοιχες καταγραφές και με τις αριθμητικές αναλύσεις που έγιναν με την *ισοδύναμη-γραμμική* μέθοδο για τις συγκεκριμένες εδαφικές συνθήκες και σεισμικές διεγέρσεις (Σχήμα 12).

Τέλος, τονίζεται ότι οι νέες σχέσεις παρουσιάζουν μεν σαφή πλεονεκτήματα ακρίβειας και ευχρηστίας σε σύγκριση με τις εμπειρικές και αριθμητικές μεθόδους αντίστοιχα, αλλά παραμένουν απλώς προσεγγιστικές και κατ' επέκταση κατάλληλες για προκαταρκτικούς μόνον υπολογισμούς της εδαφικής ενίσχυσης. Περαιτέρω, η εφαρμογή τους θα πρέπει να περιορίζεται σε περιπτώσεις όπου οι τιμές των βασικών γεωτεχνικών και σεισμολογικών παραμέτρων δεν παραβιάζουν τα αντίστοιχα όρια των δεδομένων που χρησιμοποιήθηκαν στις αριθμητικές αναλύσεις και τα οποία συνοψίζονται στον Πίνακα 1 του άρθρου.

ΕΥΧΑΡΙΣΤΙΕΣ

Η ερευνητική μας προσπάθεια χρηματοδοτήθηκε από τον Οργανισμό Αντισεισμικού Σχεδιασμού και Προστασίας (Ο.Α.Σ.Π.). Ο καθηγητής κ. Γ. Γκαζέτας συνέβαλε με χρήσιμα σχόλια επί της παρουσίασης, οι δε συνάδελφοι πολιτικοί μηχανικοί Θωμάς Πανουργιάς και Μιχάλης Κλούβας συνέβαλαν στη στατιστική επεξεργασία των δεδομένων. Επιπλέον, η επισκέπτης σπουδάστρια πολιτικός μηχανικός κα Niki Kringos (TU Delft) βοήθησε στη σύγκριση με τις πραγματικές καταγραφές. Τους ευχαριστούμε όλους θερμά.

Γεώργιος Δ. Μπουκοβάλας
Καθηγητής, Σχολή Πολιτικών Μηχανικών, Τομέας Γεωτεχνικής, Εθνικό Μετσόβιο Πολυτεχνείο.
Αχιλλέας Γ. Παπαδημητρίου
Δρ Πολιτικός Μηχανικός, Σχολή Πολιτικών Μηχανικών, Τομέας Γεωτεχνικής, Εθνικό Μετσόβιο Πολυτεχνείο.